




About the self-cleaning potential of TiO₂-TEOS treatments for heritage cementitious materials

Alessia Artale, Alberto Fregni*, Elisa Franzoni 

Dipartimento di Ingegneria Civile, Chimica, Ambientale e dei Materiali (DICAM), Università di Bologna, Via Terracini 28, Bologna 40131, Italy

ARTICLE INFO

Keywords:

Cement mortars
Anatase
Ethyl silicate
Inorganic treatments
Artificial soiling
Artificial rain
Photocatalytic

ABSTRACT

20th century architectural heritage has been exposed to increasingly aggressive environmental conditions, including pollutants and particulate matter in the atmosphere, which cause soiling on the surface and progressive deterioration. Hence, conservation has become a priority for this heritage, especially focusing on cement-based materials and concrete. In this paper, two self-cleaning TiO₂-based treatments were applied to different types of cement mortar slabs, representative of 20th century architecture. The first treatment consists of a TiO₂ nanoparticles dispersion in ethyl silicate, applied by brushing; in the second treatment, ethyl silicate was applied first and then cellulose pulp with a dispersion of TiO₂ was added. Treatments were first applied to smooth mortar slabs with aggregates of different chemical compositions. Then, the texture's effect was considered, and the treatments were applied to mortars slabs with different surface finishing mimicking the ones used in 20th century architecture. Standard laboratory tests were carried out, together with a new customized procedure designed to simulate real-world conditions, with artificial soiling and rain cycles, to evaluate the treatments' cleaning efficacy. The results allowed to assess the efficacy of the treatments and to find differences in their photocatalytic activity, regarding both superhydrophilicity and photodegradation effects, on different substrates. Moreover, the results highlight the limits of some standard testing procedures, which may not be suitable for heterogeneous substrates and irregular surfaces, and the need for new protocols.

1. Introduction

The conservation of cement-based materials has only recently received systematic attention. 20th century heritage buildings, structures, cultural landscapes and industrial sites are threatened by a general lack of awareness and recognition [1], generating a cultural and technical debate on appropriate conservation and restoration strategies. In 2010, ICOMOS (International Council on Monuments and Sites) drafted the first version of the Madrid Document, "Approaches for the Conservation of Twentieth-Century Cultural Heritage" [1] presented at the XVII ICOMOS General Assembly in Paris. The document, last updated in 2017, aims to provide international guidelines and a reference standard for the conservation of 20th century heritage buildings and sites. It emphasizes the importance of research and the development of "specific repair methods appropriate to the unique building materials and construction techniques of the twentieth century", underlining the need to study their differences from traditional historic materials before proceeding with standard investigative or restoration procedures.

Moreover, in recent years, urban expansion and industrial

development led to a dramatic increase in atmospheric, water, and soil pollution, having consequences not only on human health and ecosystems, but also on the built heritage [2]. Environmental pollution has accelerated the deterioration of architectural elements, causing both structural and aesthetic damage such as material loss or surface discolouration/darkening, due to chemical degradation or accumulation of soil and airborne particulate matter.

While national and international policies aim to reduce pollutants' emission, conservation interventions focus on minimizing damage through consolidation and surface protection [3], with self-cleaning treatments emerging as a promising strategy. Photocatalytic materials can actively protect substrates by promoting the removal or degradation of harmful agents deposited on surfaces, and preventing biofilm growth. Recent studies focused on self-cleaning coatings based on titanium dioxide (TiO₂), a semiconductor widely used since the early 1900s as a white pigment [4,5] and later investigated for its photocatalytic activity between the 1920s and 1950s [4]. Despite concerns about SO_x emissions during TiO₂ production [6], studies indicate a positive environmental impact resulting from its use as a coating and are investigating

* Corresponding author.

E-mail addresses: alessia.artale2@unibo.it (A. Artale), a.fregni@unibo.it (A. Fregni), elisa.franzoni@unibo.it (E. Franzoni).

<https://doi.org/10.1016/j.conbuildmat.2025.143735>

Received 11 June 2025; Received in revised form 4 September 2025; Accepted 21 September 2025

Available online 30 September 2025

0950-0618/© 2025 The Authors. Published by Elsevier Ltd. This is an open access article under the CC BY license (<http://creativecommons.org/licenses/by/4.0/>).

alternative production processes for TiO₂ to lower these harmful emissions [7].

Many studies now confirm that treatments containing TiO₂ nanoparticles in the anatase form, when exposed to sunlight, provide materials with self-cleaning, de-polluting, and antimicrobial properties [5,8]. Photocatalytic activity is characterized by two main effects:

- ▶ photodegradation of organic compounds via redox reactions;
- ▶ photoinduced superhydrophilicity, which enhances the removal of particulate matter by rain.

These effects occur at the same time, making it difficult to isolate their individual contributions to the overall self-cleaning effect [9].

TiO₂ nanoparticles are already used in the construction sector, for example as glass coating [7] or embedded in the cement matrix to provide self-cleaning properties to the entire structure, as in the church Dives in Misericordia in Rome, designed by the architect Richard Meier [10]. While many studies focused on the use of TiO₂ as part of cementitious mortars [11,12], the research in the context of conservation is more limited, probably because cultural heritage demands greater attention to the chemical, physical, and aesthetic compatibility of treatments with historic materials, as well as to the durability of their effects [13].

In the conservation field, the treatments consist of dispersing TiO₂ nanoparticles in a liquid medium, which may be water, a solvent, or an organic or inorganic matrix [14]. Recently proposed approaches include combining titanium dioxide with hydroxyapatite [15] or dispersing it in ethyl silicate [16], a widely used consolidant agent. Matrix selection is essential, as it enhances treatment durability by improving nanoparticle adhesion to the surface and preventing their removal by rain or wind [4, 17]. Application methods also influence treatment durability, being directly related to the amount of nanoparticles applied and their penetration depth. Among others, the most common techniques are spray application and brush application. Spray application reduces application time, but brush application is preferable to minimize environmental impact and ensure user's safety, due to the lower dispersion and inhalation of nanoparticles in working site [18].

So far, most studies focused on treatments applied to stone materials, such as marble or limestone [19–22], while tests on more porous materials, such as cement mortars and bricks, are still limited. For cementitious materials particular attention must be paid to the substrate heterogeneity: since it is a composite material, the treatment's effects may vary across the surface. Surface roughness, porosity, and binder type can influence the effectiveness of photocatalytic treatments [23, 24], and since these parameters are difficult to control and standardize, the results obtained across different studies are rarely fully comparable. The intrinsic heterogeneity of cement-based materials poses challenges not only to treatment performance and durability but also to experimental methodology. Photocatalytic activity is generally assessed through a few standardized laboratory tests widely used in TiO₂ research, including NO_x abatement or degradation of organic dyes. These are often accompanied by contact angle measurements to assess whether the surface of the treated material exhibits superhydrophilic behavior [9,25,26]. However, the standard tests used so far are designed for smooth, homogeneous, low-porosity materials, and are not necessarily suitable for more complex substrates [9].

This study aims at analysing the effects of two self-cleaning TiO₂-based treatments applied to cement mortar slabs, designed to replicate features typical of 20th-century architecture. At first, treatments were applied to smooth mortar slabs manufactured with different aggregates, isolating the contribution of their chemical composition. Then, the treatments were applied to mortar slabs with different surface finishing, introducing the factor of surface roughness. In addition to standard organic dye degradation test, a customized procedure was used to simulate real-world conditions. This included artificial soiling and rain cycles to evaluate the treatments' cleaning efficacy. In a previous work,

an investigation of the most promising matrices, titania nanoparticles and application methods were carried out, highlighting the treatments with greatest potential [27]. In this paper, the accelerated soiling test previously developed was changed and improved to make it more realistic in simulating soiling accumulation and removal by rain. A systematic evaluation of the discoloration and the self-cleaning ability was also carried out in this study (Fig. 1).

The aim is not only to evaluate the treatments' effectiveness and the factors influencing the photocatalytic activity over cement mortars samples, but also to highlight the limitations of current testing methods in terms of applicability and representativity when applied to heterogeneous and irregular substrates.

2. Materials and methods

2.1. Substrates

Two different types of substrates were produced, i.e., smooth mortar slabs and rough mortar slabs, with the aim of reproducing the features of typical historical cement mortars. The high porosity related to a poor manufacturing technique [16] was obtained using a relatively high w/c ratio (0.6) in all the mixes. The presence of texturized surface finishing was obtained in rough slabs by different mechanical treatments.

At first, treatments were applied to smooth slabs with different aggregates, to analyse the effects of chemical composition of the material. In fact, one aggregate is fully quartzitic and the other one is mostly carbonatic. This is expected to cover the typical composition of aggregates in real mortars. Then, tests were repeated on rough slabs, to study how the surface texture might affect the test results. Roughness generally increases the adhesive effect over surfaces by mechanical interlocking [28–31], so it can have an influence on both the treatment and the soiling retention. However, it can also result in uneven distribution or localized accumulation.

2.1.1. Smooth slabs

Smooth cement mortar slabs were manufactured to investigate the behaviour of the treatments in presence of different chemical composition of the substrate, while neglecting the issue of surface roughness. Two kinds of mortars were prepared to manufacture the smooth slabs (Fig. 2):

- Samples C1, having the following formulation:
 - 1350 g standard quartz sand, according to EN 196–1:2016 [32];
 - 450 g CEM II/A-LL 32.5 R;
 - 270 g deionized water.
- Samples C2, having the following formulation:
 - 953 g standard quartz sand, according to EN 196–1:2016 [32];
 - 397 g limestone gravel, with $1 \leq d \leq 3.5$ mm;
 - 450 g CEM II/A-LL 32.5 R;
 - 270 g deionized water.

The mortars were prepared in a Hobart mixer, cast and cured for 28 days according to the procedure in EN 196–1, producing $4 \times 4 \times 16$ cm³ mortar prisms. After curing, the prisms were cut by sawing, producing $4 \times 4 \times 0.5$ cm³ specimens for testing. The specimens were let cure in laboratory conditions for additional one year to allow a complete carbonation of the mortars, as in historic structures.

2.1.2. Rough slabs

As one of the main purposes of the newly developed treatments is to obtain a self-cleaning behaviour on the texturized cement-based materials of 20th century heritage, rough mortar slabs were prepared too. The purpose here was to manufacture a range of mortars with different features also in terms of surface roughness. The following samples were prepared:

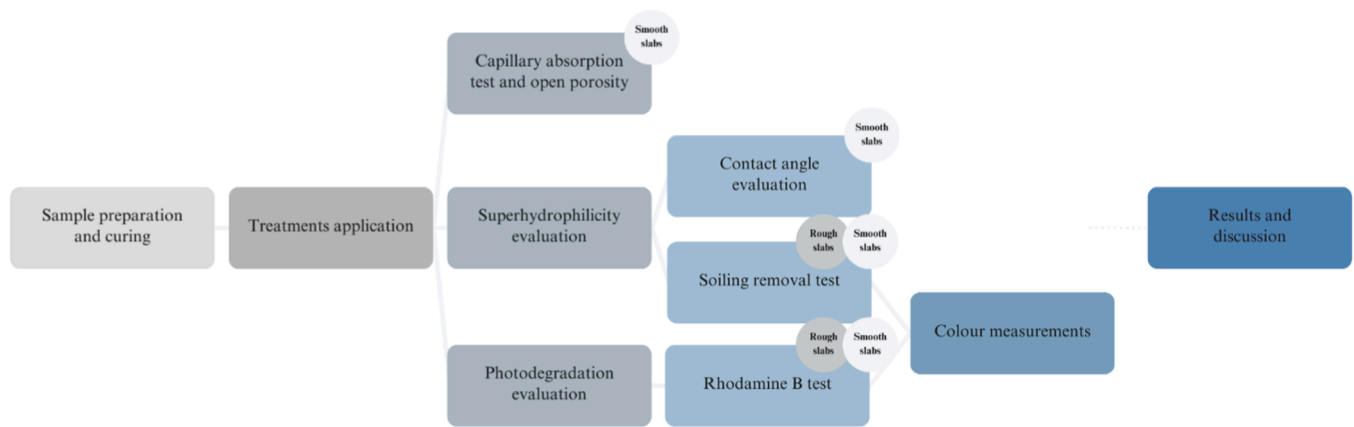


Fig. 1. Workflow of the experimental sequence.

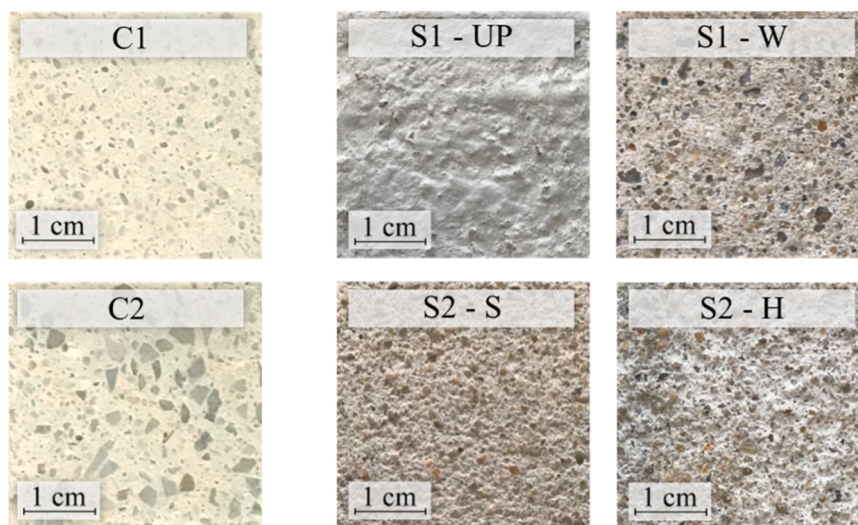


Fig. 2. Aspect of mortar samples' surface: smooth slabs (C1-C2) and rough slabs (S1-S2) with different surface finishing (UP = unpolished; W = washed; S = sandpapered; H = hammered).

- Samples S1:
 - 953 g standard quartz sand, according to EN 196–1:2016 [32];
 - 397 g limestone gravel ($1 \leq d \leq 3.5$ mm);
 - 450 g CEM II/A-LL 32.5 R;
 - 270 g deionised water.
- Samples S2:
 - 1350 g standard quartz sand, according to EN 196–1:2016 [32];
 - 450 g CEM II/A-LL 42.5 R;
 - 270 g deionised water.

The mortars were cast into moulds having size $15 \times 12 \times 2$ cm³ and immediately compacted and levelled by a trowel. After curing for 24 h in a humid chamber (temperature $20 \pm 2^\circ\text{C}$ and relative humidity $> 95\%$), the samples' surfaces were made rough through one of the following procedures:

- ▶ washing with high pressure tap water (label W)
- ▶ sandpapering (label S)
- ▶ hammering (label H)

while some samples were left unpolished (label UP), for comparison's sake.

In particular the following samples were produced: S1-UP, S1-W, S2-S, S2-H (Fig. 2). Two slabs for each condition were manufactured. All the

slabs were let cure for further 1 year in lab conditions.

2.2. Treatments

Two different treatments were used in this research, both based on the combination of Tetraethyl Orthosilicate (TEOS) and TiO₂ nanoparticles. The first treatment (labelled as TR1) was prepared dispersing 3 % TiO₂ nanoparticles (75 % anatase and 25 % rutile, Aeroxide TiO₂ P25) in TEOS (ethyl silicate oligomers in 25 % white spirit, ESTEL 1000, CTS Italia). This treatment was applied to each sample by two orthogonal brush strokes [33]. After the treatment was absorbed, the samples were wrapped in Parafilm for 24 h to prevent evaporation and then unwrapped and let cure in laboratory environment for 4 weeks. The second treatment (labelled as TR2) consisted in a 2-step application. Firstly, the same TEOS used in TR1 was applied to the slabs by brushing, with four orthogonal brush strokes, then each sample was immediately covered with a homogeneous layer (about 5 mm) of cellulose pulp with a TiO₂ dispersion. This poultice was constituted by cellulose pulp and a commercial dispersion of TiO₂ nanoparticles in ethanol (Colorobbia AT-20-SG01, 3 wt% dispersion). The weight ratio between cellulose pulp and dispersion was 1:7. Application with poultice is not common as brushing, but can be used to achieve a higher consolidant absorption [34,35]. The samples were immediately wrapped in Parafilm. After 48 h, the film was removed and the samples were rinsed with deionized

water. The slabs were then left uncovered for 4 weeks to allow for the hardening reactions of ethyl silicate.

After 28 days, the treated surfaces were qualitatively tested by releasing water drops over the, to assess possible residual hydrophobicity. As the surface was still slightly hydrophobic, indicating that the TEOS condensation reactions were not complete yet, the samples were immersed in deionised water for 24 h to allow the hardening reactions complete. Finally, the samples were dried in ventilated oven at 60°C for 24 h before any further testing, as this temperature is not expected to affect TiO₂ or TEOS structure [36–38].

Among all forty smooth slabs, twenty of type "C1" and twenty of type "C2", sixteen of each type were treated (eight with TR1 and eight with TR2) while four slabs were left untreated (samples UT), for comparison. In the case of the rough slabs, two specimens were available for each of the 4 conditions. In that case, to allow a direct comparison of the treated and untreated surface, one specimen was half treated with TR1 and the other specimen was half treated with TR2. The remaining two halves were used as untreated references.

2.3. Methods

The methods applied for the experimentation are summarized in Table 1. For rough slabs, Rhodamine B degradation test and soiling removal test were performed on all samples as shown in Fig. 3.

2.3.1. Capillary absorption and open porosity

The capillary absorption test was performed on the smooth slabs only, to observe any differences in absorption rate between treated and untreated materials. The test was carried out according to EN 15801:2009 [39]. In brief, the dry slabs (mass m_{dry}) with the treated face downwards were placed over a layer of absorbent paper continuously soaked with deionized water, and then weighed at fixed time intervals. The capillary water absorption rate, i.e. the amount of water absorbed per unit surface area over the square root of time was calculated, according to the mentioned standard. After one hour, the slabs were completely submerged in water for 5 h. Then, the samples were extracted, gently dried on the surface and the saturated surface-dry mass was measured (m_{sat}).

Finally, hydrostatic weighing of the samples was performed, thus calculating the open porosity (PA%) and bulk density (ρ_g), as:

$$PA\% = \frac{m_{sat} - m_{dry}}{m_{sat} - m_{hydro}} \cdot 100$$

$$\rho_g = \frac{m_{dry}}{m_{sat} - m_{hydro}} \cdot \rho_{water}$$

where:

- ▶ m_{dry} is the dry mass
- ▶ m_{sat} is the saturated surface-dry mass
- ▶ m_{hydro} is saturated mass from hydrostatic weighing
- ▶ ρ_{water} is water density.

The measurement of capillary absorption and porosity was not

Table 1
Experimental design.

Mortar type	Treatment	Testing methods
C1, C2 (smooth slabs)	UT	▶ Capillary absorption test and open porosity
	TR1	▶ Contact angle evaluation
	TR2	▶ Rhodamine B degradation test ▶ Soiling removal test
S1-UP, S1-W, S2-S, S2-H (rough slabs)	UT	▶ Rhodamine B degradation test
	TR1	▶ Soiling removal test
	TR2	▶ Soiling removal test

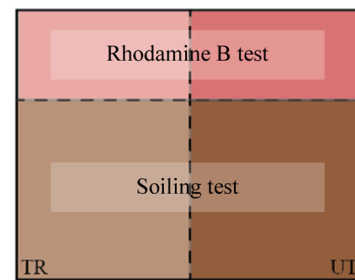


Fig. 3. Schematic division of the slabs (treated half on the left, untreated half on the right): the upper part in pink was used for the Rhodamine test, while the lower part was dedicated to the soiling removal test.

carried out on the rough slabs, as they include in the same sample both treated and untreated areas.

2.3.2. Contact angle

The hydrophilicity of the treated and untreated surfaces was investigated on the smooth slabs, by measuring the contact angle [19,40]. In fact, the surface roughness could disrupt the droplet, making a reliable angle measurement impossible. Static contact angle was measured by a DSA30S (Krüss, Germany), in five different points for each sample. Before the test, the samples were left under UV lamps for five hours to allow activation of the superhydrophilic effect.

2.3.3. Rhodamine B degradation test

The photocatalytic activity of the treatments was assessed through the photodegradation of an organic compound [9,25,26]. This test was performed on both smooth and rough slabs. For the rough ones, surface was ideally divided into different parts, in order to perform all the planned tests on the same sample including the soiling removal test (par. 2.3.4).

This laboratory test is one of the most used to evaluate the photocatalytic activity of surfaces [20,41]. Following UNI 11259:2016 [42], an aqueous solution containing 0.1 g/L of Rhodamine B was prepared, and approximately 3.5 mL of it were released by a pipette over the surface of each sample. The slabs were left in the dark for twenty-four hours and then placed under UV lamps up to 4 and 24 h. The discolouration was quantified by a portable spectrophotometer (3nh NH310 Portable Colorimeter), which provides the result in CIE 1976 L*a*b* coordinates (L^* , a^* , b^*) [43]. The chromatic difference between two points or conditions (ΔE) is measured as:

$$\Delta E = \sqrt{\Delta L^{*2} + \Delta a^{*2} + \Delta b^{*2}}$$

where:

- ▶ L^* represents lightness, ranging from 0 (black) to 100 (white);
- ▶ a^* represents the variation from green (negative values) to red (positive values);
- ▶ b^* represents the variation from blue (negative values) to yellow (positive values).

A threshold of 3 for ΔE is usually considered for the chromatic difference to be visible to human eye.

Cementitious mortar samples do not have a homogeneous colour surface, and the presence of aggregates makes colour evaluation very difficult. To overcome this problem, a plastic template with a paper mask with nine holes was manufactured for the smooth slabs (Fig. 4a-b). This allowed to measure colour coordinates quickly and on the same points on the samples throughout the test, yielding comparable data for discolouration assessment. For the rough slabs, after securing their position, the masks with the nine holes were placed on top for the same purpose (Fig. 4c-d).

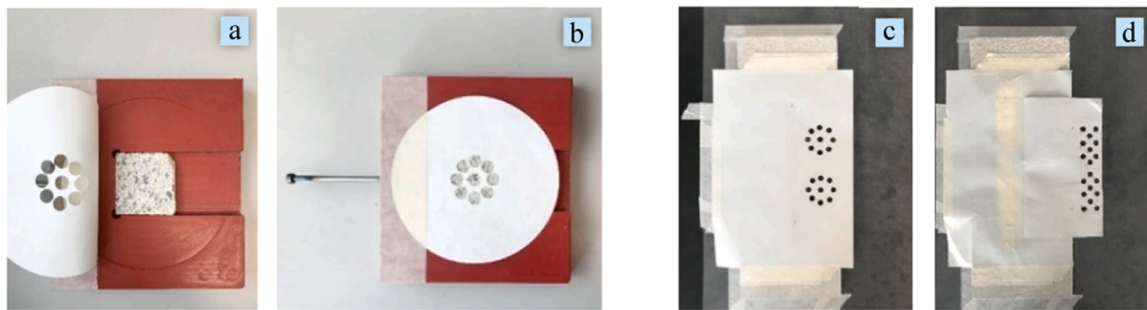


Fig. 4. Template for colorimetric investigations on smooth slabs (a-b) and template for investigations on rough slabs (c-d).

Since Rhodamine is a red dye, the UNI 11259:2016 standard suggests considering only the variation of the a^* coordinate when assessing the discolouration rate, according to two parameters:

$$\begin{aligned} \blacktriangleright R_4 &= \frac{a^*(0h) - a^*(4h)}{a^*(0h)} \times 100 \\ \blacktriangleright R_{24} &= \frac{a^*(0h) - a^*(24h)}{a^*(0h)} \times 100 \end{aligned}$$

where $a^*(xh)$ is the a^* coordinate after x hours of UV exposure.

According to the standard, it should be:

$$\begin{aligned} \blacktriangleright R_4 &\geq 20 \% \\ \blacktriangleright R_{24} &\geq 50 \% \end{aligned}$$

for the surface to be considered photocatalytic.

However, it must be noted that the standard UNI 11259:2016 neglects the possibility that the initial a^* coordinate is different from zero. In this study, since the starting value of a^* of the unstained samples was not zero, the adapted formula suggested in a study on the photocatalytic effects of TiO_2 on travertine [20] was preferred. Thus, the two parameters were normalized with respect to the original appearance (a^* coordinate) of samples before the application of Rhodamine, according to the following formulas:

$$\begin{aligned} \blacktriangleright R^*_4 &= \frac{a^*(0h) - a^*(4h)}{a^*(0h) - a^*} \times 100 \\ \blacktriangleright R^*_{24} &= \frac{a^*(0h) - a^*(24h)}{a^*(0h) - a^*} \times 100 \end{aligned}$$

where $a^*(xh)$ is the a^* coordinate after x hours of UV exposure, and a^* is the a^* coordinate before the application of Rhodamine. The 20 % and 50 % threshold values are still valid for the assessment of photocatalytic activity.

2.3.4. Soiling removal test

Photoinduced superhydrophilicity is expected to contribute to the removal of particulate matter, keeping the surface clean and accessible to UV rays from solar radiation, which also activate the decomposition reactions of organic compounds. If the surface is superhydrophilic, the contact angle with water approaches zero and the droplet spreads, creating a thin layer between the surface and the dirt, thereby facilitating particulate removal.

The procedure to investigate the effectiveness of materials' self-cleaning ability is not standardized and references in the literature are lacking. In fact, many studies testing photocatalytic activity use degradation tests of Rhodamine B, methylene blue, or other organic dyes (par. 2.3.3), but these procedures highlight only the contribution of redox reactions to compound degradation, and not that of superhydrophilicity in dirt removal. On the other hand, the measurement of the contact angle (par. 2.3.2) is very common for the assessment of materials' superhydrophilicity, but without considering its specific contribution to particulate washout.

For this reason, an innovative procedure was used in this study,

following the first successful tests reported in [27]. The procedure was applied to sixteen smooth slabs and to a part of the rough slabs (Fig. 3). Firstly, the samples were sprayed with a dispersion simulating the soiling on a façade exposed to an urban environment and then they were subjected to cycles of brief UV exposure and washing, mimicking the effect of rain. Colour measurements were performed using a spectrophotometer during the test (par. 2.3.3).

The procedure can be schematically divided into three phases, as shown in Table 2.

In urban environments, external surfaces accumulate soiling agents that are both natural (marine aerosols, wind-blown dust from rocks, soil, vegetation, etc.) and anthropogenic (from the combustion of fossil fuels and biomass, vehicle emissions and heating systems). Based on this, the ASTM International standard D7897 - 18 [44] developed an aqueous dispersion with dissolved salts, dust, and carbonaceous particulate to simulate three years of soiling, as required for the evaluation of solar reflectance and thermal emissivity. Although the purpose of the artificial soiling proposed in the ASTM standard is different from that of the present study, the same mix was adopted for the evaluation of the soiling removal capacity. However, as this dispersion produced only a minor darkening on the investigated samples, the amounts of the different components of the dispersion were increased 30 times, leading to the following composition of the artificial soiling:

- Dust: Fe_2O_3 : 3 g/L; Montmorillonite: 20 g/L 61 %
- Salts: NaCl: 3 g/L; NaNO_3 : 3 g/L; $\text{CaSO}_4 \cdot 2 \text{H}_2\text{O}$: 4 g/L 31 %
- Soot: Aqua-Black 001 (commercial): 13.7 g/L 8 %

The dispersion was sprayed over the samples (placed horizontally) by an airbrush at 1.4 bar pressure, kept about 25 cm above the sample, moving the airbrush to cover the entire surface uniformly. After soiling deposition, each slab was placed under an infrared lamp for about ten minutes to make the water evaporate. Once dry, the colour of each sample was measured by spectrophotometry.

To evaluate the effectiveness of treatments in facilitating the mechanical washing of particulate matter, a process was designed to

Table 2
Stages of the test for soiling removal.

Stages of soiling removal test	
Contamination	Contamination of samples with an artificial soiling dispersion and drying under infrared lamp Measurement of colorimetric coordinates UV light exposure for 1 h
Artificial Rain Cycles ($\times 2$)	Measurement of colorimetric coordinates Spraying of water for cleaning Drying of samples in oven at 60°C for 24 h Measurement of colorimetric coordinates UV light exposure for 4 h
Final UV Exposure	Measurement of colorimetric coordinates UV light exposure for additional 22 h Measurement of colorimetric coordinates

simulate the effect of rain on the treated surface after brief UV exposure to activate superhydrophilicity. The samples were exposed to UV light (OSRAM DULUX S blue UVA, 9 W) for one hour, and then colorimetric coordinates were measured. Then, the slabs were positioned vertically on a grid and washed by spraying with nebulized deionized water. To ensure uniform and consistent washing across the surface, a pressure pump was maintained at constant pressure during the test.

For each sample simulated rain was applied: a total of 100 mL over smooth samples, corresponding to about 6 mL/cm², and a total of 600 mL over rough slabs, corresponding to about 10 mL/cm². After washing, the samples were oven dried at 60°C for 24 h, and colorimetric coordinates were measured again. The entire washing cycle was repeated twice. After completing this part of the test, which was strongly related to the assessment of the role of materials' superhydrophilicity, all soiled samples were placed under UV lamps for 24 h to check for any possible additional photodegradation.

The procedure followed to evaluate the colour change was the same used also for Rhodamine test (par. 2.3.3). Colorimetric investigations were conducted according to the mentioned standard, after 4 and then 24 h of exposure.

3. Results and discussion

3.1. Smooth slabs

3.1.1. Capillary absorption and open porosity

The slabs' capillary absorption coefficients (AC) are shown in Fig. 5. The treatments slightly slowed down the absorption process. This is likely due to a partially blocking of pores near the surface caused by the consolidant, but the reduction of AC was so limited that it does not suggest any compatibility issues, but rather a positive impact on the mortars' durability. Notably, the super-hydrophilicity of TiO₂ caused no negative effect in terms of increased water absorption speed, which could cause several deterioration mechanisms with potentially detrimental effect. Among the untreated samples, C1 exhibited a higher AC than C2, while for the treated samples there were no significant differences in absorption behaviour based on the aggregate type. In the capillary absorption test, all the untreated samples reached saturation in less than 15 min, whereas the treated samples took between 20 and 25 min.

Consistently, the open porosity is quite uniform across all samples, with slightly higher values for the untreated ones (Table 3).

3.1.2. Contact angle evaluation

The contact angle measurement revealed not so high differences between treated and untreated samples. However, the specimens displayed quite scattered behaviours, making it difficult to derive quantitative observation in terms of contact angles. In fact, cement mortars are heterogeneous, thus the water droplet can fall either on aggregates or on the cementitious matrix, which have different surface texture and

Table 3

Open porosity (%) of the untreated and treated smooth samples.

Substrate	Open porosity [%]		
	UT	TR1	TR2
C1	16.2 ± 0.4	15.1 ± 0.6	15.9 ± 0.8
C2	16.4 ± 0.5	15.5 ± 0.4	16.1 ± 0.2

porosity, resulting in different contact angles. Moreover, the cementitious slabs, even if considered smooth, inherently exhibit small imperfections making the droplet break. Hence, the droplet has an irregular profile and the contact angle varies along its perimeter. For all these reasons, the results of this test were evaluated only qualitatively, as a complement to the other tests. In general, the treated slabs (especially those with the treatment TR1) exhibit lower contact angles with respect to the untreated ones, as shown in the examples in Fig. 6.

This is an interesting occurrence, which indicates that the surface is made more hydrophobic by the presence of TiO₂ (as desired for the self-cleaning effect), but the capillary water absorption is not increased (as desired for durability, see 3.1.1). This means that the effect of the consolidant is preponderant below the surface, as expected.

3.1.3. Rhodamine B degradation test

The degradation of rhodamine under UV and the subsequent discoloration were very limited in the untreated slabs, especially in C1 substrate, as shown in Fig. 7 (R*₄ and R*₂₄).

On the contrary, the treated samples exhibited high discoloration percentages, especially in the samples containing quartz sand (C1), even considering higher standard deviations. For these slabs, the values exceeded the threshold set by UNI 11259:2016 standard, namely 20 % discoloration after 4 h of UV radiation and 50 % after 24 h, while the samples with fine aggregate exceeded the first threshold after 4 h but not the second one. No particular difference was noticed in the discoloration for the two treatments. The better performance of the treatments on C1 samples was attributed to the better adhesion of TEOS matrix onto quartz sand than on limestone gravel [45].

Since the open porosity and capillary absorption coefficients are very similar across all treated samples (par. 3.1.1), it can be concluded that the chemical nature of the substrate and in particular the aggregate strongly influences the effectiveness of the photocatalytic action.

3.1.4. Soiling removal test

Table 4 reports the ΔE of the different steps of the test for the artificial soiling removal, while the total ΔE measured for the samples in all these steps is reported in Fig. 8. Considering that visual assessment of the self-cleaning effect corresponds to ΔE ≥ 3, the results reported in the table and figure allow to make some observations. The discoloration caused by the first exposure to UV was slightly higher in the treated samples than in the untreated one, but in all cases very limited, indicating that the compounds present in the artificial soiling are not

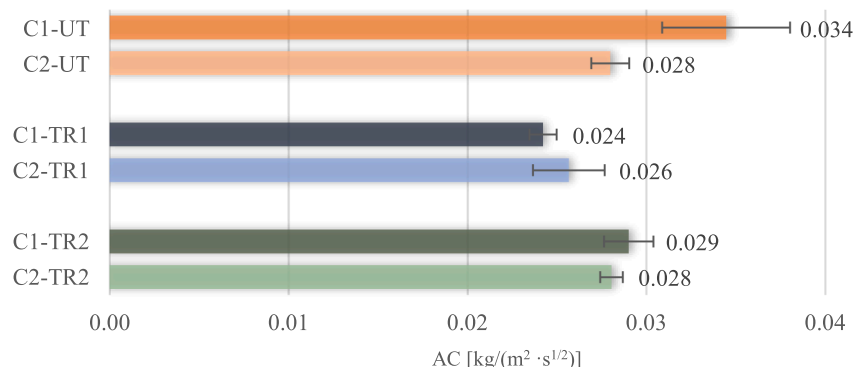


Fig. 5. Capillary absorption coefficient (AC) of the smooth mortar samples.

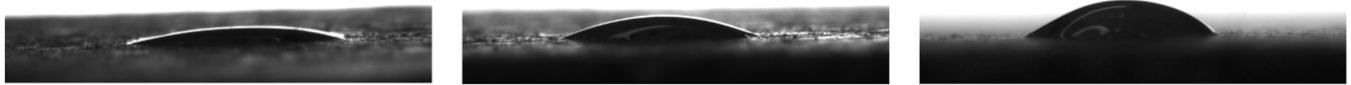


Fig. 6. Some significant photos of samples C2 with TR1 (left), TR2 (centre), and untreated (right).

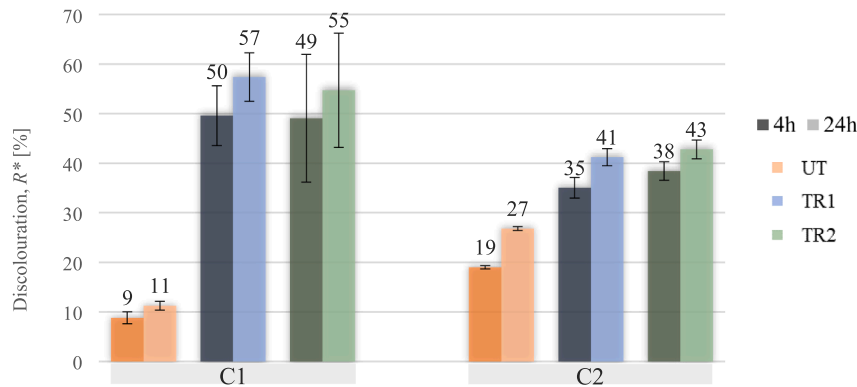


Fig. 7. Discolouration R* of the smooth slabs during the rhodamine degradation test.

Table 4

Average ΔE [-] of the different steps of the test for the artificial soiling removal on smooth slabs.

	Cycle I		-	Cycle II		-	Cumulative cycles I+II	-	UV	
	UV - 1 h	Washing		UV - 1 h	Washing				UV - 4 h	UV - 24 h
C1-UT	0.34 ± 0.11	2.27 ± 1.30		0.36 ± 0.05	0.88 ± 0.21		3.30 ± 1.67		0.54 ± 0.08	0.37 ± 0.04
C1-TR1	0.61 ± 0.17	6.31 ± 1.66		0.38 ± 0.17	1.04 ± 0.36		7.81 ± 1.28		0.62 ± 0.11	0.43 ± 0.07
C1-TR2	0.42 ± 0.03	8.86 ± 1.06		0.32 ± 0.08	1.44 ± 0.38		10.55 ± 0.85		0.70 ± 0.20	0.41 ± 0.07
C2-UT	0.33 ± 0.06	3.26 ± 0.18		0.36 ± 0.07	0.54 ± 0.07		3.62 ± 0.38		0.47 ± 0.03	0.34 ± 0.09
C2-TR1	0.58 ± 0.35	9.74 ± 0.27		0.38 ± 0.08	1.08 ± 0.18		11.28 ± 0.15		0.60 ± 0.08	0.32 ± 0.05
C2-TR2	0.40 ± 0.09	8.45 ± 1.50		0.34 ± 0.07	1.29 ± 1.42		10.00 ± 2.82		0.49 ± 0.12	0.36 ± 0.03

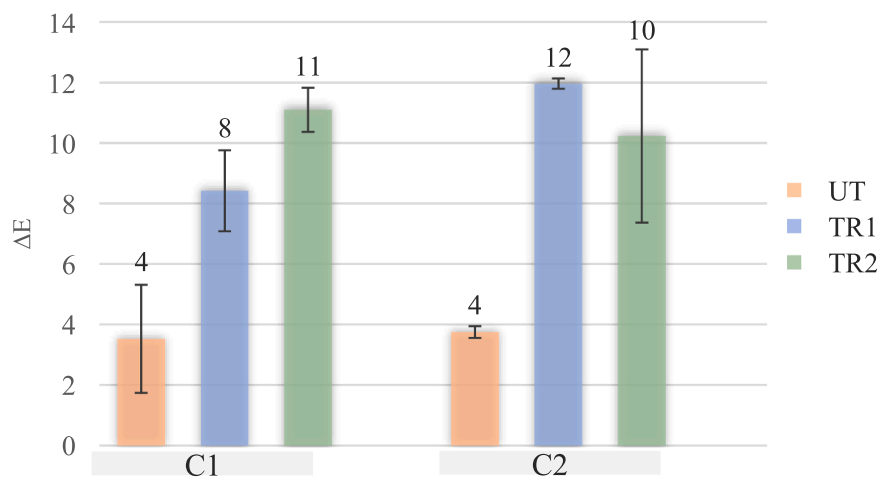


Fig. 8. Total ΔE measured for the samples at the end of the soiling removal test (two water nebulization stages).

degradable through simple redox reactions, or at least not within the timeframe of this test. It was the first washing cycle that yielded clearly visible results, while the additional effect of the second washing was very limited, likely because all removable particulate matter had already been eliminated in the first cycle. The two cycles of washing caused a ΔE in the untreated samples equal to 3.3 for C1 and 3.6 for C2, while the treated samples exhibited almost triple values, reaching an average ΔE of 9.5 for the first treatment and ΔE of 10.3 for the second. Hence, the treatments clearly promoted the washing away of the artificial soiling. The final UV exposure did not cause any significant discolouration, for

the same reasons reported above.

Overall, the ΔE values in the treated samples are significantly higher than those in the untreated ones, however the soiling was not completely removed, even in the slabs with the highest ΔE . This is likely due, primarily, to the porosity of the samples, which may have absorbed the artificial soiling to a certain depth, not reached by UV rays. As the treatments partially blocked the surface pores, this effect could be more evident in the untreated samples (more porous), while the untreated ones may have benefited from an easier washing of particulate matter, along with the photoinduced superhydrophilicity of the titanium

dioxide-based treatments.

It can also be noticed that the effectiveness of TR1 was higher in substrate C2, while the effectiveness of TR2 was higher in substrate C1. Standard deviations reach high values in some cases, probably due to the heterogeneity of the cement mortars. However, since the numbers of point investigated for each sample was high, the trend of the results obtained can still be clearly observed.

According to ASTM International standard D7897 - 18 for photovoltaic cells, the artificial soiling applied over the samples corresponded to the effect of ninety years of dirt accumulation, while the washing procedure adopted in the test corresponded to a light rain, which was anyway effective in removing at least the first layer of soiling. Considering that the time interval occurring in practice between two successive rains is certainly shorter than ninety years, the results obtained can be considered very promising.

3.2. Rough slabs

3.2.1. Rhodamine B degradation test

The following graph (Fig. 9) shows the percentage discolouration of rhodamine after 4 and 24 h of UV exposure, calculated averaging the measurements in the nine selected points for each sample. All the treated parts of the samples showed good results, with discolouration percentages exceeding 60 % in almost all cases after just the first four hours, in a uniform manner, regardless the type of surface texture or treatment applied. In the untreated parts of the slabs, the degradation of rhodamine led to low or undetectable discolouration, and in most cases the a^* value even seems to increase during the test. This may be related, on the one hand, to the difficulty in measuring very low colour differences in a so heterogeneous surface and, on the other hand, to the fact that the substrate is not white like marble, but has its own colour, which can influence the assessment of discolouration according to the a^* coordinate, as previously noticed. As for smooth slabs, higher standard deviations values can be attributed to the heterogeneity of the mortar samples and they do not impede to observe the trend of the results obtained.

3.2.2. Soiling removal test

Fig. 10 and Table 5 show that similarly to what found for the smooth slabs, only the first washing cycle was effective in terms of artificial

soiling removal. Whereas the untreated areas exhibited barely visible ΔE values, all the treated ones reached a colour difference above the threshold of 3. The overall ΔE values, evaluated considering the complete test, are shown in Fig. 10. Although the measured ΔE values prove a clear difference between treated and untreated sections, with a beneficial effect deriving from the treatments, these values are relatively low, especially if compared to the smooth slabs. The roughness of the samples made it more difficult to wash away the dirt, as expected. This is primarily due to the irregular morphology, which increases the contact area and promotes adhesion by mechanical interlocking. However other mechanisms should be considered, such as capillary absorption or changes in interfacial tension, which could have affected pollutants' removal.

Comparing the treatments, TR1 seems more effective than TR2 in promoting the soiling removal, in three of the four substrates. Interestingly, the type of surface texture seems to lead to no particular differences in the self-cleaning effectiveness of the treatments, which is positive because the treatments seem "robust" enough to be not so affected by the roughness of the mortar substrate.

Like in the smooth slabs, the dirt was only partially removed and in this case the effect can be ascribed to the fact that the slabs exhibited a significant capillary absorption rate, causing a partial soiling penetration to depths where UV rays could not activate the treatment. By the way, the mixture used for the artificial soiling was adapted from one used to simulate the soiling on photovoltaic panels, for which porosity is not an issue.

As for the smooth substrates, the second washing cycle did not result in any visible outcome, hence the results seem independent from the amount of water used. This can be considered a very encouraging result, because it suggests that the removal of soiling does not necessarily require high amounts of rain.

As highlighted in the results of the test performed on the smooth slabs, a light simulated rain proved to be effective in removing the most superficial layer and would likely be enough to remove the layer of dirt that, under real conditions, deposits on a surface in the time interval between two successive rains.

4. Conclusions

The objective of this research was to evaluate the effectiveness of two

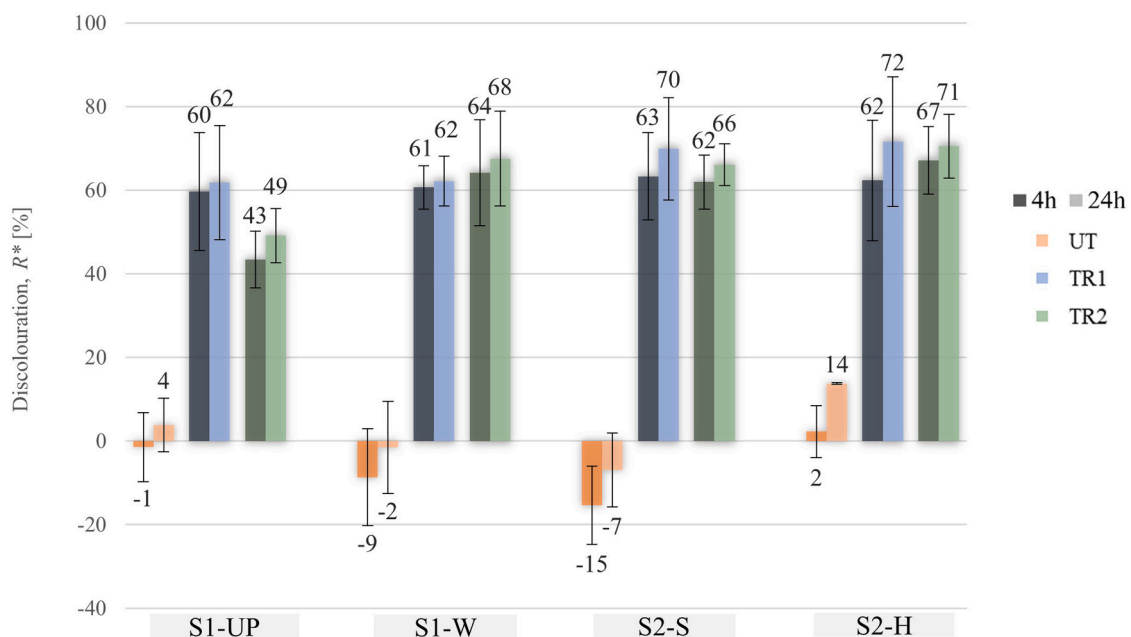


Fig. 9. Discolouration R^* of the rough slabs during the rhodamine degradation test.

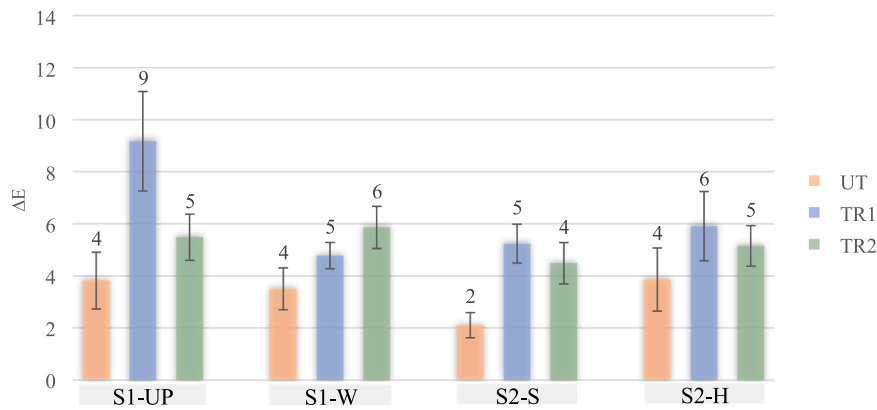


Fig. 10. Total ΔE measured for the samples at the end of the soiling removal test.

Table 5

Average ΔE [-] of the different steps of the test for the artificial soiling removal on rough slabs.

	Cycle I		Cycle II	
	UV - 1 h	Washing	UV - 1 h	Washing
S1-UP-UT	0.33 ± 0.09	2.98 ± 0.18	0.35 ± 0.12	1.08 ± 0.45
S1-UP-TR1	0.31 ± 0.21	6.34 ± 1.12	1.53 ± 1.27	1.65 ± 0.71
S1-UP-TR2	0.37 ± 0.18	4.83 ± 0.65	0.44 ± 0.17	0.57 ± 0.28
S1-W-UT	0.32 ± 0.15	2.08 ± 0.15	0.27 ± 0.03	1.56 ± 0.38
S1-W-TR1	0.36 ± 0.15	4.25 ± 0.76	0.43 ± 0.26	0.48 ± 0.18
S1-W-TR2	0.41 ± 0.21	4.22 ± 0.62	0.85 ± 0.97	1.96 ± 0.34
S2-S-UT	0.39 ± 0.07	1.33 ± 0.13	0.38 ± 0.02	0.95 ± 0.18
S2-S-TR1	0.41 ± 0.27	4.71 ± 0.73	0.55 ± 0.46	0.40 ± 0.20
S2-S-TR2	0.28 ± 0.18	3.61 ± 0.80	0.52 ± 0.26	0.55 ± 0.32
S2-H-UT	0.54 ± 0.13	3.27 ± 0.47	0.47 ± 0.06	0.43 ± 0.05
S2-H-TR1	0.28 ± 0.09	5.46 ± 1.19	0.63 ± 0.28	0.38 ± 0.27
S2-H-TR2	0.80 ± 0.30	5.00 ± 0.87	0.62 ± 0.20	0.51 ± 0.28

self-cleaning TiO_2 -based treatments, applied to different cement mortar slabs, using different testing procedures. Two application methods were compared: TEOS and TiO_2 applied separately, using a commercial TiO_2 alcoholic suspension already tested in previous experiments [27], and TEOS and TiO_2 applied together in a single solution, to test the feasibility of a solvent-free treatment. The choice of these two different application strategies was made to evaluate not only the performance of the treatments, but also the possibility of combining environmental sustainability with effectiveness. The results allow to conclude that the application of the studied treatments provide cement mortar with photocatalytic behaviour. It can be observed that there are no systematic or significant differences between the two treatments, so TiO_2 and ethyl silicate can be combined into a single treatment without basically affecting the photocatalytic activity.

The treatments reduce only slightly the water capillary absorption rate of the samples, which was ascribed to a slight porosity reduction owing to TEOS consolidant: this may reduce the penetration of rain, substances and particulate matter into the material's porosity without causing a pore blocking effect.

A high percentage of TiO_2 (3 wt%) was used in the tests: since the photocatalytic activity of this type of treatment was confirmed, lower TiO_2 concentrations will be investigated in the next phases, also to reduce the slight whitening which was visually observed over the samples.

Regarding the tests on smooth slabs, it was demonstrated that photocatalytic activity depends on the chemical composition of the substrate, although not in a systematic way.

- The capillary absorption test revealed that the treatments levelled out the differences in open porosity among slabs with different

aggregates, indicating that the variations in photocatalytic activity are linked to the chemical nature of the substrate.

- In the soiling removal test the treatments helped the water to wash the soiling away. TR1 yielded better results on quartz slabs, whereas TR2 was more effective on samples with limestone aggregate. The cleaning action was due to water, while UV rays played a role only in activating the superhydrophilicity of the treatments.
- Regardless of the treatment type, the rhodamine B test showed higher discolouration percentages in the slabs with limestone aggregate, although in all cases the treated samples exhibited significantly greater discolouration than untreated ones. Most of the discolouration occurred in the first four hours of UV exposure.

For the rough slabs, the following observations can be made:

- In the soiling removal test, the discolouration of the treated areas was greater than that of untreated parts but less visible than in the smooth slabs. The roughness of the samples made it more difficult to remove soiling, which remained anchored in the surface irregularities. No significant differences were observed based on the type of surface roughness, but in general, the first treatment demonstrated greater effectiveness. Again, the only effect of UV exposure was activating superhydrophilicity, without directly contributing to dirt removal.
- The rhodamine B test results were positive and consistent for both treatments and for all the surfaces. Also in this case, discolouration mainly occurred within the first four hours, reaching 60 % in nearly all cases.

During the tests some methodological difficulties emerged, related to the procedures followed and their application to porous and heterogeneous substrates. The standard prescribed for the rhodamine B test was not particularly suitable for cementitious substrates, which are heterogeneous and absorbing. Due to the high porosity of the samples, rhodamine was not retained on the surface but instead was absorbed deeply and unevenly. On the other hand, the newly proposed test also presents some limitations. First, the soiling removal was carried out only through water, without mechanical action: this created difficulties, particularly on rough slabs, where dirt remained attached to surface imperfections. Furthermore, the test simulates ninety years of accumulated dirt without any cleaning. Conversely real rainfall events are characterised by alternate deposition and washout phases, so probably the test should be modified to take into account more realistic exposure condition. It is clear that this test was designed to emphasize soiling deposition and rainfall events, but the resulting procedure was probably too severe.

Based on these considerations, the treatments yielded good results. However, further investigations are necessary to clarify which substrate

characteristics most significantly influence photocatalytic activity. Finally, particular attention should be paid to the procedures currently in use to adapt them to more heterogeneous materials and to the real exposure conditions of these materials in contemporary urban contexts.

CRedit authorship contribution statement

Elisa Franzoni: Writing – review & editing, Visualization, Validation, Supervision, Methodology, Formal analysis, Conceptualization. **Alberto Fregni:** Writing – review & editing, Visualization, Validation, Supervision, Methodology, Investigation, Formal analysis, Data curation, Conceptualization. **Alessia Artale:** Writing – review & editing, Writing – original draft, Visualization, Validation, Methodology, Investigation, Formal analysis, Data curation.

Declaration of Competing Interest

The authors declare that they have no known competing financial interests or personal relationships that could have appeared to influence the work reported in this paper.

Data availability

The authors are unable or have chosen not to specify which data has been used.

References

- ICOMOS International Scientific Committee on Twentieth Century Heritage, Madrid-New Delhi Document “Approaches to the Conservation of Twentieth-century Cultural Heritage,” 2017. ISBN 978-2-918086-63-5.
- E. Sesana, A.S. Gagnon, C. Ciantelli, J.A. Cassar, J.J. Hughes, Climate change impacts on cultural heritage: a literature review, *WIREs Clim. Change* 12 (2021) e710, <https://doi.org/10.1002/wcc.710>.
- C. Galli, *Indicazioni ed elaborati grafici per il progetto di restauro architettonico*, Liguori, Napoli, 2009.
- E. Franzoni, A. Fregni, R. Gabrielli, G. Graziani, E. Sassoni, Compatibility of photocatalytic TiO₂-based finishing for renders in architectural restoration: a preliminary study, *Build. Environ.* 80 (2014) 125–135, <https://doi.org/10.1016/j.buildenv.2014.05.027>.
- J. Chen, C. Sun Poon, Photocatalytic construction and building materials: from fundamentals to applications, *Build. Environ.* 44 (2009) 1899–1906, <https://doi.org/10.1016/j.buildenv.2009.01.002>.
- Commission Decision 2009/544/EC of 13 August 2008 establishing ecological criteria for the award of the Community eco-label to indoor paints and varnishes, *Official Journal of the European Union*, 2008.
- H. Babaizadeh, M. Hassan, Life cycle assessment of nano-sized titanium dioxide coating on residential windows, *Constr. Build. Mater.* 40 (2013) 314–321, <https://doi.org/10.1016/j.conbuildmat.2012.09.083>.
- E. Jimenez-Relinque, J.R. Rodriguez-Garcia, A. Castillo, M. Castellote, Characteristics and efficiency of photocatalytic cementitious materials: type of binder, roughness and microstructure, *Cem. Concr. Res.* 71 (2015) 124–131, <https://doi.org/10.1016/j.cemconres.2015.02.003>.
- F. Hamidi, F. Aslani, TiO₂-based photocatalytic cementitious composites: materials, properties, influential parameters, and assessment techniques, *Nanomaterials* 9 (2019) 1014, <https://doi.org/10.3390/nano9101444>.
- L. Cardellicchio, On conservation issues of contemporary architecture: the technical design development and the ageing process of the jubilee church in Rome by richard meier, *Front. Archit. Res.* 7 (2018) 107–121, <https://doi.org/10.1016/j.foar.2018.03.005>.
- J.H. Atta-ur-Rehman, H.G. Kim, A. Kim, J.S. Qudoos, Ryou, Effect of leaching on the hardened, microstructural and self-cleaning characteristics of titanium dioxide containing cement mortars, *Constr. Build. Mater.* 207 (2019) 640–650, <https://doi.org/10.1016/j.conbuildmat.2019.02.170>.
- M. Sumesh, U.J. Alengaram, M.Z. Jumaat, K.H. Mo, M.F. Alnahhal, Incorporation of nano-materials in cement composite and geopolymer based paste and mortar – a review, *Constr. Build. Mater.* 148 (2017) 62–84, <https://doi.org/10.1016/j.conbuildmat.2017.04.206>.
- E. Franzoni, R. Gabrielli, E. Sassoni, A. Fregni, G. Graziani, N. Roveri, E. D’Amen, Performance and permanence of TiO₂-based surface treatments for architectural heritage: Some experimental findings from on-site and laboratory testing, in: J. Hughes, T. Howind (Eds.), *Science and Art: A Future for Stone: Proceedings of the 13th International Congress on the Deterioration and Conservation of Stone*, University of the West of Scotland, Paisley, UK, 2016, Vol. 2, pp. 761–768. ISBN 978-1-903978-58-0.
- E. Franzoni, M.C. Bignozzi, E. Rambaldi, TiO₂ in building sector, in: F. Parrino, L. Palmisano (Eds.), *Metal Oxides, Titanium Dioxide (TiO₂) and Its Applications*, Elsevier, 2021, pp. 449–479.
- E. Sassoni, E. D’Amen, N. Roveri, G.W. Scherer, E. Franzoni, Durable self-cleaning coatings for architectural surfaces by incorporation of TiO₂ nanoparticles into hydroxyapatite films, *Materials* 11 (2018) 177, <https://doi.org/10.3390/ma11020177>.
- C. Pizzigatti, Solutions for the conservation and restoration of cement-based materials in XX century architectural heritage, PhD Thesis, Alma Mater Studiorum - University of Bologna, 2022..
- L. Graziani, E. Quagliarini, F. Bondioli, M. D’Orazio, Durability of self-cleaning TiO₂ coatings on fired clay brick façades: effects of UV exposure and wet & dry cycles, *Build. Environ.* 71 (2014) 193–203, <https://doi.org/10.1016/j.buildenv.2013.10.005>.
- R. Kaegi, et al., Synthetic TiO₂ nanoparticle emission from exterior facades into the aquatic environment, *Environ. Pollut.* 156 (2008) 233–239, <https://doi.org/10.1016/j.envpol.2008.08.004>.
- E. Quagliarini, F. Bondioli, G.B. Goffredo, A. Licciulli, P. Munafò, Self-cleaning materials on architectural heritage: compatibility of photo-induced hydrophilicity of TiO₂ coatings on stone surfaces, *J. Cult. Herit.* 14 (2013) 1–7, <https://doi.org/10.1016/j.culher.2012.02.006>.
- E. Quagliarini, F. Bondioli, G.B. Goffredo, C. Cordoni, P. Munafò, Self-cleaning and de-polluting stone surfaces: TiO₂ nanoparticles for limestone, *Constr. Build. Mater.* 37 (2012) 51–57, <https://doi.org/10.1016/j.conbuildmat.2012.07.006>.
- E. Quagliarini, F. Bondioli, G.B. Goffredo, A. Licciulli, P. Munafò, Smart surfaces for architectural heritage: preliminary results about the application of TiO₂-based coatings on travertine, *J. Cult. Herit.* 13 (2012) 204–209, <https://doi.org/10.1016/j.culher.2011.10.002>.
- P. Munafò, G.B. Goffredo, E. Quagliarini, TiO₂-based nanocoatings for preserving architectural stone surfaces: an overview, *Constr. Build. Mater.* 91 (2015) 31–44, <https://doi.org/10.1016/j.conbuildmat.2015.02.083>.
- E. Jimenez-Relinque, J.R. Rodriguez-Garcia, A. Castillo, M. Castellote, Characteristics and efficiency of photocatalytic cementitious materials: type of binder, roughness and microstructure, *Cem. Concr. Res.* 71 (2015) 124–131, <https://doi.org/10.1016/j.cemconres.2015.02.003>.
- J. Hot, J. Topalov, E. Ringot, A. Bertron, Investigation on parameters affecting the effectiveness of photocatalytic functional coatings to degrade NO: TiO₂ amount on surface, illumination, and substrate roughness (Article ID), *Int. J. Photo* 2017 (2017) 6241615, <https://doi.org/10.1155/2017/6241615>.
- CNR, The European project PICADA: Study of titanium dioxide as photocatalyst for a new class of building materials, 2024. <https://www.cnr.it/en/focus/101-2/the-european-project-picada-study-of-titanium-dioxide-as-photocatalyst-for-a-new-class-of-building-materials> (accessed February 2024).
- ISO 10678:2010, Fine ceramics (advanced ceramics, advanced technical ceramics) - Determination of photocatalytic activity of surfaces in an aqueous medium by degradation of methylene blue, International Organization for Standardization, 2010.
- E. Franzoni, C. Pizzigatti, R. Fabris, Developing inorganic coatings with nano-TiO₂ for heritage concrete and assessing their self-cleaning performance by a new laboratory test, *Constr. Build. Mater.* 449 (2024) 138282, <https://doi.org/10.1016/j.conbuildmat.2024.138282>.
- K. Davaasambuu, Y. Dong, A. Pramanik, A.K. Basak, Mechanisms and performance of composite joints through adhesive and interlocking means—A review, *J. Compos. Sci.* 9 (2025) 359, <https://doi.org/10.3390/jcs9070359>.
- H. Wei, J. Xia, W. Zhou, L. Zhou, G. Hussain, Q. Li, K.K. Ostrikov, Adhesion and cohesion of epoxy-based industrial composite coatings, *Compos. B Eng.* 193 (2020) 108035, <https://doi.org/10.1016/j.compositesb.2020.108035>.
- L. Graziani, E. Quagliarini, A. Osimani, L. Aquilanti, F. Clementi, C. Yéprémian, V. Lariccia, S. Amoroso, M. D’Orazio, Evaluation of inhibitory effect of TiO₂ nanocoatings against microalgal growth on clay brick façades under weak UV exposure conditions, *Build. Environ.* 64 (2013) 38–45, <https://doi.org/10.1016/j.buildenv.2013.03.003>.
- L. Graziani, E. Quagliarini, M. D’Orazio, The role of roughness and porosity on the self-cleaning and anti-biofouling efficiency of TiO₂-Cu and TiO₂-Ag nanocoatings applied on fired bricks, *Constr. Build. Mater.* 129 (2016) 116–124, <https://doi.org/10.1016/j.conbuildmat.2016.10.111>.
- EN 196-1:2016, *Methods of Testing Cement - Part 1: Determination of Strength*, European Committee for Standardization, 2016.
- A. Fregni, L. Venturi, E. Franzoni, Evaluation of the performance and durability of self-cleaning treatments based on TiO₂ nanoparticles applied to cement-based renders and boards, *Coatings* 13 (2023) 990, <https://doi.org/10.3390/coatings13060990>.
- E. Franzoni, E. Sassoni, G. Graziani, Brushing, poultice or immersion? The role of the application technique on the performance of a novel hydroxyapatite-based consolidating treatment for limestone, *J. Cult. Herit.* 16 (2015) 173–184, <https://doi.org/10.1016/j.culher.2014.05.009>.
- D. Mudronja, F. Vanmeert, K. Hellemans, S. Fazinic, K. Janssens, D. Tibiljas, M. Rogosic, S. Jakovljevic, Efficiency of applying ammonium oxalate for protection of monumental limestone by poultice, immersion and brushing methods, *Appl. Phys. A* 111 (2013) 109–119, <https://doi.org/10.1007/s00339-012-7365-9>.
- S.B. Desu, Decomposition chemistry of tetraethoxysilane, *J. Am. Ceram. Soc.* 72 (1989) 1615–1621, <https://doi.org/10.1111/j.1151-2916.1989.tb06292.x>.
- M.G.M. van der Vis, E.H.P. Cordfunke, R.J.M. Konings, The thermodynamic properties of tetraethoxysilane (TEOS) and an infrared study of its thermal decomposition, *J. Phys. IV Proc.* 3 (1993) C3-75–C3-82, <https://doi.org/10.1051/jp4:1993309>.

- [38] S. Jamil, M. Fasehullah, Effect of temperature on structure, morphology, and optical properties of TiO₂, *Mater. Int* 1 (2021) 21–28, <https://doi.org/10.54738/MI.2021.1103>.
- [39] EN 15801:2009, Conservation of Cultural Property - Test Methods - Determination of Water Absorption by Capillarity, European Committee for Standardization, 2009.
- [40] N. Sakai, A. Fujishima, T. Watanabe, K. Hashimoto, Quantitative evaluation of the photoinduced hydrophilic conversion properties of TiO₂ thin film surfaces by the reciprocal of contact angle, *J. Phys. Chem. B* 107 (2003) 1028–1035, <https://doi.org/10.1021/jp022105p>.
- [41] S. Faisal, A. Kumar Patra, Investigation on photocatalytic and structural characteristics of normal concrete using TiO₂ at ambient temperature, *Mater. Today Proc.* 68 (2022) 164–173, <https://doi.org/10.1016/J.MATPR.2022.08.425>.
- [42] UNI 11259:2016, Fotocatalisi - determinazione dell'attività fotocatalitica di leganti idraulici. Metodo della rodamina, Ente Nazionale Italiano di Unificazione, 2016.
- [43] UNI EN ISO/CIE 11664-4:2019, Colorimetria - Parte 4: Spazio colore L*a*b* CIE 1976, Ente Nazionale Italiano di Unificazione, 2019.
- [44] ASTM D7897 - 18, Standard practice for laboratory soiling and weathering of roofing materials to simulate effects of natural exposure on solar reflectance and thermal emittance, ASTM International, 2018.
- [45] G.W. Scherer, G. Wheeler, Silicate consolidants for stone, *Key Eng. Mater.* 391 (2008) 1–25, <https://doi.org/10.4028/www.scientific.net/kem.391.1>.